ELSEVIER

Journal of Nuclear Materials 299 (2001) 205–218

journal of nuclear materials

www.elsevier.com/locate/jnucmat

Effect of neutron irradiation and post-irradiation annealing on microstructure and mechanical properties of OFHC-copper

B.N. Singh [a,*], D.J. Edwards [b], P. Toft [a]

[a] *Materials Research Department, Risø National Laboratory, DK-4000 Roskilde, Denmark*
[b] *Structural Materials Development, Pacific Northwest National Laboratory, P.O. Box 999, Richland, WA 99352, USA*

Received 17 April 2001; accepted 14 September 2001

Abstract

Specimens of oxygen-free high conductivity (OFHC) copper were irradiated in the DR-3 reactor at Risø at 100 °C to doses in the range 0.01–0.3 dpa (NRT). Some of the specimens were tensile tested in the as-irradiated condition at 100 °C whereas others were given a post-irradiation annealing treatment at 300 °C for 50 h and subsequently tested at 100 °C. The microstructure of specimens was characterized in the as-irradiated as well as irradiated and annealed conditions both before and after tensile deformation. While the interstitial loop microstructure coarsens with irradiation dose, no significant changes were observed in the population of stacking fault tetrahedra (SFT). The post-irradiation annealing leads to only a partial recovery and the level of recovery depends on the irradiation dose level. However, the post-irradiation annealing eliminates the yield drop and reinstates enough uniform elongation to render the material useful again. These results are discussed in terms of the cascade-induced source hardening (CISH) model.

1. Introduction

It is well established that neutron irradiation at temperatures below the recovery stage V (i.e. $<0.4T_m$ where T_m is the melting temperature) causes a substantial amount of hardening and a severe reduction in the ductility of metals and alloys. Furthermore, the irradiated materials generally lose their ability to deform homogeneously and to work-harden and suffer from plastic instability (i.e. yield drop and flow localization). This behaviour has been observed in fcc, bcc and hcp metals and alloys (see [1,2] for recent reviews). The irradiation-induced loss of ductility as well as plastic instability are matters of serious concern from the point of view of performance and lifetime of materials used in the structural components of fission or fusion reactors.

Traditionally, the magnitude of irradiation-induced hardening has been treated within the framework of the 'Zone Theory' of radiation hardening originally proposed by Seeger [3]. Seeger assumed that vacancy-rich zones created by displacement cascade events created impenetrable obstacles that were by-passed by the bowing of dislocation segments around them, in essence proposing a modified form of the Orowan model [4]. This approach has been further modified over the years to become the more commonly known dispersed barrier hardening (DBH) model, where the increase in yield strength is proportional to the square root of the product of the average size and density of obstacles such as dislocation loops, stacking fault tetrahedra (SFT), cavities, and other features formed during irradiation. However, in the case of irradiated materials containing weak, shearable obstacles in the form of small loops and SFT the applicability of the DBH model has been

* Corresponding author. Tel.: +45-46 775 709; fax: +45-46 775 758.
E-mail address: bachu.singh@risoe.dk (B.N. Singh).

0022-3115/01/$ - see front matter
PII: S0022-3115(01)00698-5

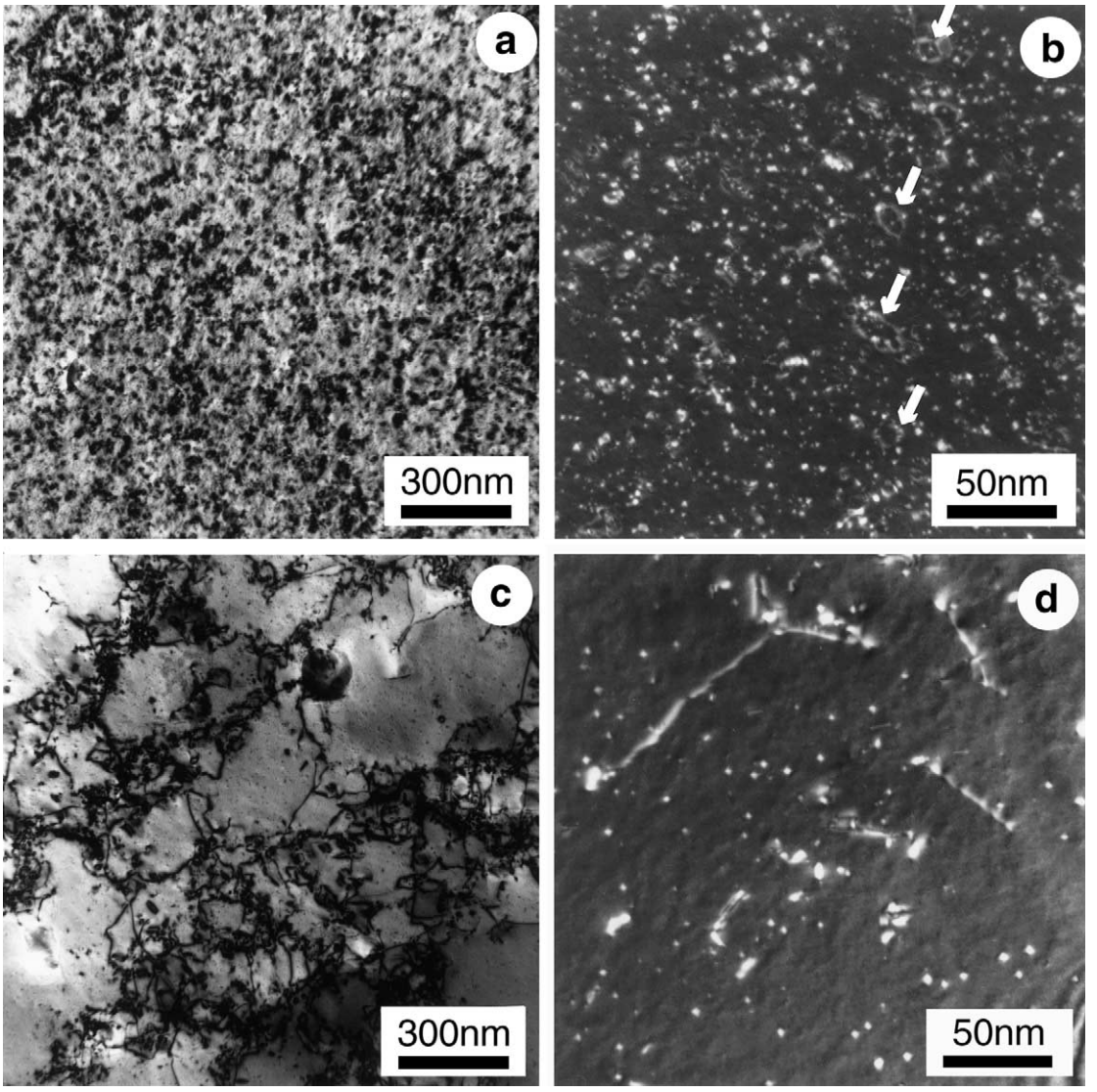

Fig. 1. Loop and SFT microstructures of copper irradiated at 100 °C to 0.01 dpa: (a) loops; (b) SFT in the as-irradiated condition and (c) loops and dislocations; (d) SFT after post-irradiation annealing at 300 °C for 50 h.

questioned recently [1]. As described by Singh et al. [1], the DBH model is unable to predict the experimental observations of yield drop and the subsequent flow localization that often occurs in these materials tested at temperatures below the recovery stage V.

To overcome these problems, Singh et al. [1] proposed the 'cascade-induced source hardening' (CISH) model which can rationalize not only the increase in the yield stress but also the observations of yield drop and plastic flow localization. The main thesis of this model is that during irradiation under cascade damage conditions, the grown-in dislocations get decorated by one-dimensionally migrating clusters of self-interstitial atoms (SIAs). The experimental evidence for such dislocation decoration and the formation of rafts of SIA clusters during neutron irradiation has been reviewed by Trinkaus et al. [5,6]. Furthermore, it has been established by detailed analytical calculations that the phenomena of dislocation decoration as well as raft formation can be understood only in terms of one-dimensional glide of SIA clusters [5,6]. These phenomena have been further investigated using three-dimensional dislocation dynamics [7,8] and molecular dynamics [9,10] simulations. The results of these computer simulations fully corroborate the results of the analytical calculations [5,6]. In analogy with Cottrell atmosphere [11], the decoration effectively pins the dislocations and prevents them from acting as dislocation sources until

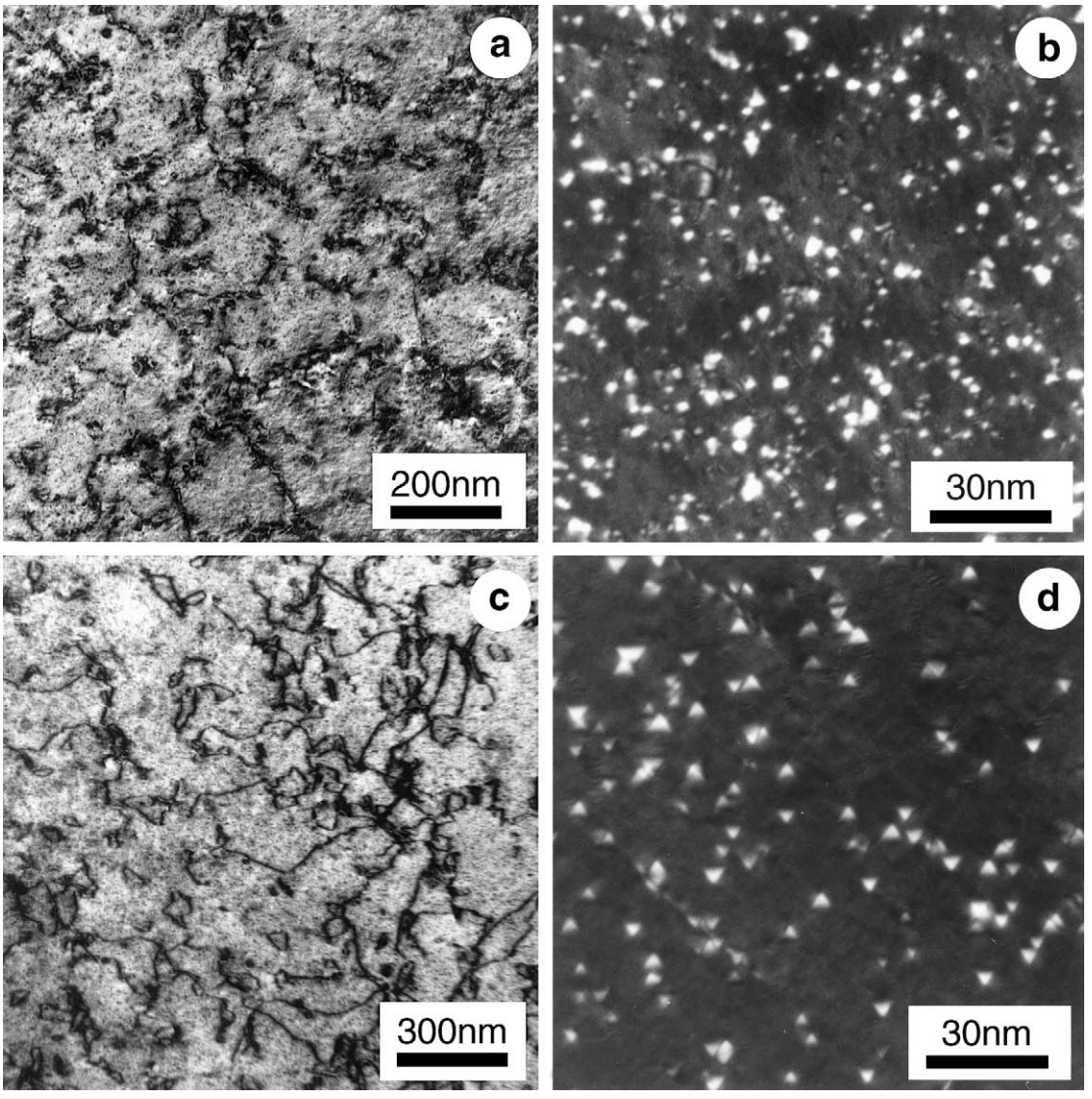

Fig. 2. Loop and SFT microstructures of copper irradiated at 100 °C to 0.1 dpa: (a) loops and raft-like agglomerates of loops; (b) SFT in the as-irradiated condition and (c) large loops and dislocation segments; (d) SFT after post-irradiation annealing at 300 °C for 50 h.

the applied stress reaches a high enough level to 'free' the dislocations from the atmosphere of clusters and loops decorating them. In the CISH model this stress level refers to the upper yield stress. At this high stress level, dislocations are likely to be released from the moderately decorated dislocations and points of stress/strain singularities (e.g. surfaces, interfaces, grain boundaries, inclusions, etc.). These sites of dislocation generation are most likely to be the sites where the formation of 'cleared channels' begins.

Thus, according to the CISH model, the occurrence of the yield drop and plastic flow localization can be prevented by removing the atmosphere of loops decorating the grown-in dislocations. This can, at least in principle, be achieved by post-irradiation annealing at or above the recovery stage V. The population of interstitial loops decorating the dislocations may anneal out by the flux of vacancies, may get absorbed into the dislocations or may coalesce by glide or conservative climb during the annealing. Since small SFT formed during irradiation are expected to emit vacancies during annealing at temperature above the recovery stage V, it is reasonable to speculate that the dense population of SFT will become the main source of the vacancy flux reaching the loops decorating the grown-in dislocations. Furthermore, the glide and climb of the small SIA

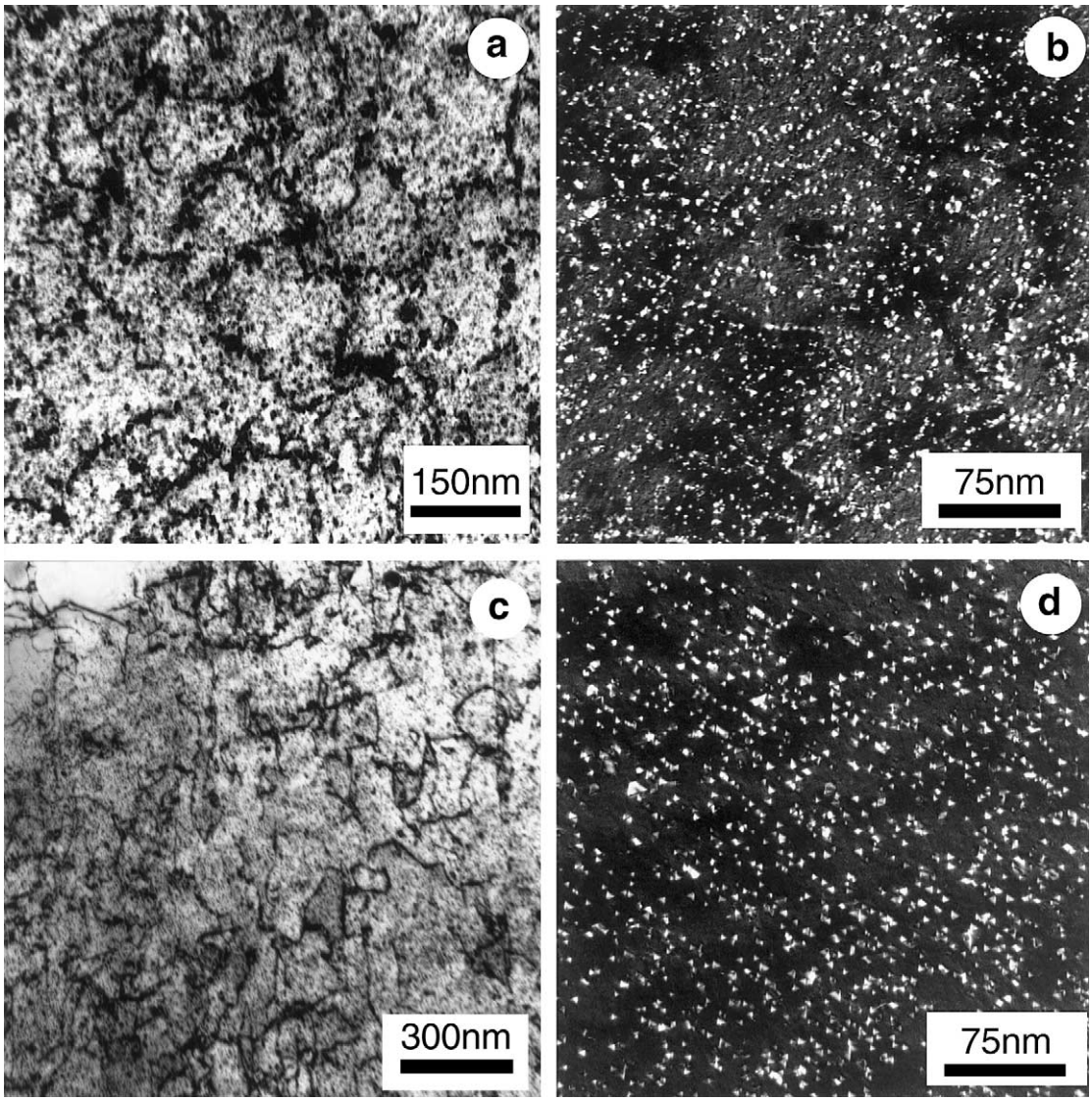

Fig. 3. Loop and SFT microstructures of copper irradiated at 100 °C to 0.3 dpa: (a) loops and raft-like agglomerates of loops; (b) SFT in the as-irradiated condition or (c) loops, dislocation segments and loose network; (d) SFT after post-irradiation annealing at 300 °C for 50 h.

clusters during annealing are likely to coarsen the SIA clusters/loops in the matrix and to contribute to the shrinkage of the SFT population. Consequently, a decrease in the hardening level and an increase in the ductility can be expected. This raises the possibility that in-service annealings during reactor shutdowns might alleviate the problem of yield drop and flow localization and may increase the service lifetime of the respective components.

It should be pointed out that the effects of post-irradiation annealing on the yield stress of copper were studied already in the 1960s (e.g. see [12,13]). However, most of these experiments were limited to only low doses and did not address the problem of yield drop and plastic flow localization. Furthermore, in microstructural characterization, no distinctions were made between the interstitial (loop) and vacancy (SFT) components of the microstructure. In addition, in these earlier investigations no attempts were made to determine the correlation between the as-irradiated and post-irradiation annealed microstructures before and after mechanical testing.

In the present investigations of the effect of post-irradiation annealing, this correlation has been studied systematically. In addition, the dose dependence of the evolution of both interstitial and vacancy components of

the microstructure has been determined. The results of transmission electron microscopy (TEM) on the as-irradiated and irradiated and annealed oxygen-free high conductivity (OFHC) copper specimens irradiated to different doses are described in Section 3.1 and the corresponding tensile properties are presented in Section 3.2. The post-deformation microstructures of both as-irradiated and post-irradiation annealed OFHC-copper specimens are illustrated in Section 3.3. The results are discussed in Section 4. The main conclusions emerging from the present results and their analysis are briefly summarized in Section 5.

It is relevant to mention here that the corresponding effects of post-irradiation annealing on the electrical resistivity (conductivity) of the specimens studied in the present investigations are described in [14].

2. Materials and experimental procedure

The material used in the present investigation was thin (0.3 mm) sheet of OFHC-copper containing 10, 3, <1 and <1 ppm, respectively, of Ag, Si, Fe and Mg. The oxygen content of this copper was found to be 34 appm.

Tensile samples of OFHC-copper were irradiated in the DR-3 reactor at Risø National Laboratory. Prior to irradiation, the OHFC copper samples were annealed at 550 °C for 2 h in a vacuum of 10^{-9} bar. The resulting grain size and dislocation density were about 30 μm and $\leqslant 10^{12}$ m^{-2}, respectively. The tensile specimens were irradiated at 100 °C to different dose levels in the range 0.01–0.3 dpa (NRT). All specimens were irradiated with a displacement damage rate of $\simeq 5 \times 10^{-8}$ dpa (NRT)/s. A subset of the irradiated specimens were given a post-irradiation annealing treatment of 300 °C for 50 h under vacuum ($<10^{-9}$ bar). Unirradiated, as-irradiated and post-irradiation annealed specimens were tensile tested in an Instron machine at a strain rate of 1.2×10^{-3} s^{-1}. Tensile tests were carried out at 100 °C in vacuum ($<10^{-7}$ bar). The test temperature of 100 °C was reached within 30 min.

Characterization of the microstructure of the various samples was performed using a JEOL 2000FX transmission electron microscope (TEM). Both unirradiated and irradiated specimens were twin-jet electropolished in a solution of 25% perchloric acid, 25% ethanol and 50% water at 11 V for about 15 s at ~20 °C. The post-deformation microstructure of the as-irradiated and post-irradiation annealed samples were also investigated. For these investigations, 3 mm discs were punched out of the gauge length of tensile specimens after they had fractured during tensile tests. These discs were taken from the portion of the gauge length closest to the fracture surface and electropolished for TEM investigations. A JEOL 840 scanning electron microscope was used to characterize the fracture surfaces.

3. Experimental results

3.1. As-irradiated and irradiated and annealed microstructures

The microstructure of the as-irradiated specimens irradiated to all four displacement doses was found to be dominated by the presence of a high density of small SFTs homogeneously distributed throughout the grains. However, the microstructure also contained a much lower density of small dislocation loops. Furthermore, raft-like agglomerates of loops were observed at lower magnifications in thicker areas. These loops and their agglomerates are found to respond strongly both to irradiation dose and post-irradiation annealing at 300 °C for 50 h. Although we have not determined the character of these small loops, we surmise that they are of interstitial-type (see later). The evolution of loop, dislocation and SFT microstructures as a function of displacement dose and post-irradiation annealing is illustrated in Figs. 1–3.

Fig. 1(a) and (b) shows the as-irradiated microstructure for the specimens irradiated to a dose level of 0.01 dpa. The low magnification micrograph (Fig. 1(a)) clearly illustrates that the specimen irradiated to 0.01 dpa contains a modest density ($\sim 5 \times 10^{21}$ m^{-3}) of small resolvable loops of about 10 nm in diameter and are homogeneously distributed. The density of these loops, however, is likely to be an underestimate since some of the interstitial loops and SIA clusters are likely to glide to the surface of the thin foil due to image forces. Fig. 1(b) shows the high magnification micrograph demonstrating the presence of small SFTs, as well as some of the small resolvable loops (marked by arrows). The size distribution of these SFTs is presented in Fig. 4 whereas their mean size is quoted in Table 1.

The low and high magnification micrographs of the specimen irradiated to 0.01 dpa and then annealed at 300 °C for 50 h are shown in Fig. 1(c) and (d), respectively. The fact that the annealing has a dramatic effect on the as-irradiated microstructure is demonstratably clear. The microstructure shown in Fig. 1(c) clearly suggests that a considerable amount of migration and coalescence of the small loops (Fig. 1(a)) must have taken place during annealing at 300 °C. This transformation of the microstructure also supports our assumption that the small loops are of interstitial-type. A comparison of Fig. 1(b) and (d) clearly demonstrates that a very large fraction of SFTs formed during irradiation have annealed out during annealing at 300 °C. The size distribution of the SFTs after annealing is shown in Fig. 4 and their mean size is presented in Table 1.

Fig. 2 shows the low and high magnification micrographs of specimens irradiated to 0.1 dpa (Fig. 2(a) and (b)) and subsequently annealed at 300 °C for 50 h

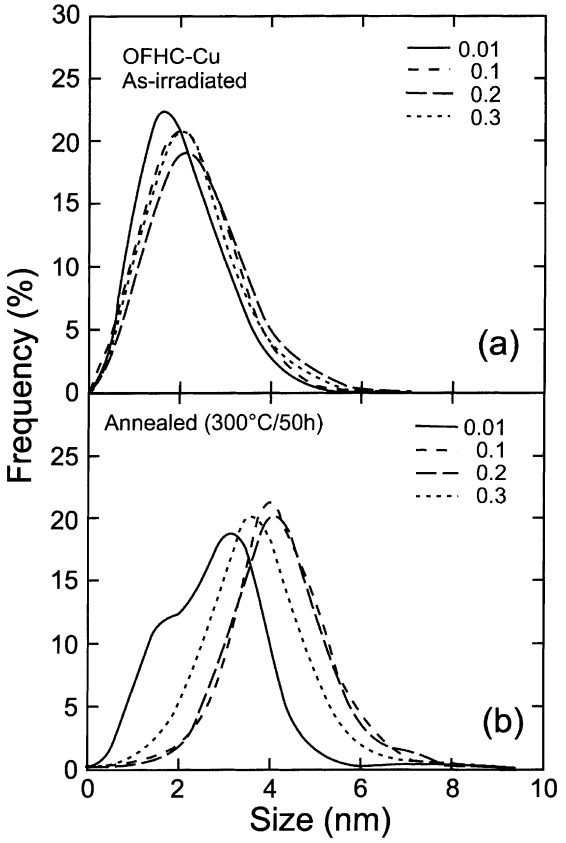

Fig. 4. Size distributions of SFT in copper irradiated at 100 °C to different doses in the (a) as-irradiated condition and (b) after post-irradiation annealing at 300 °C for 50 h. Note that the broadening of the size distribution due to annealing is sensitive to the irradiation dose (i.e. the microstructure prior to annealing).

(Fig. 2(c) and (d)). A comparison of Fig. 1(a) and Fig. 2(a) shows that the continued irradiation from 0.01 to 0.1 dpa causes significant changes in the resulting microstructure. The increase in the dose from 0.01 to 0.1 dpa leads to agglomeration and coarsening of the small loops. Furthermore, already at this dose level, the agglomerates of loops begin to form a kind of a network (Fig. 2(a)). These agglomerates of loops are, in many ways, akin to rafts of loops observed in bcc metals (e.g. [15]). As can be seen in Table 1, the SFT density increases noticeably with increasing dose but the mean SFT size remains almost unaltered. Fig. 2(c) and (d) shows low and high magnification micrographs of specimens irradiated (to 0.1 dpa) and subsequently annealed at 300 °C for 50 h. As can be seen in Fig. 2(c), this annealing treatment leads to further coarsening of the loop microstructure. Furthermore, in some local areas a few dislocation segments and a loose network of dislocation segments are formed (Fig. 2(c)). The SFT microstructures for the as-irradiated as well as for the irradiated and annealed specimens are shown in Fig. 2(b) and (d), respectively. The corresponding size distributions of SFTs are shown in Fig. 4 and the density and size are quoted in Table 1.

Fig. 3 shows both the low and the high magnification micrographs of specimens irradiated to 0.3 dpa in the as-irradiated and irradiated and annealed conditions. As can be seen in Fig. 3(a), the agglomerates of loops (i.e. raft-like structure) have, in general, become somewhat thicker compared to the ones at 0.1 dpa (Fig. 2(a)). After annealing at 300 °C for 50 h, the microstructure contains a relatively high density of dislocation segments ($\simeq 3 \times 10^{14}$ m^{-2}) and a very few interstitial loops and their agglomerates. A similar density of dislocation segments was found in specimens irradiated to 0.2 dpa at 100 °C and then annealed at 300 °C for 50 h. Some of these segments are in the form of loose networks (Fig. 3(c)). It should be pointed out that some of the dislocation segments still (i.e. even after annealing) appear to be decorated with small loops. The SFT microstructures for both as-irradiated and irradiated and annealed specimens are shown in Fig. 3(b) and (d), respectively. The SFT size distributions are presented in Fig. 4 and the mean size and density of SFTs are quoted in Table 1.

Table 1
Average size (d_S) and number density (c_S) of SFTs and number of vacancies (N_V) contained in the SFTs in the as-irradiated and post-irradiation annealed OFHC-copper

Dose (dpa)	Average size (nm)	Density (10^{23} m^{-3})	N_V (10^{25} m^{-3})	$\sqrt{c_S d_S}$ (10^7 m^{-1})
As-irradiated (at 100 °C)				
0.01	2.3	2.4	1.7	2.4
0.1	2.4	4.5	3.4	3.3
0.2	2.6	4.5	3.9	3.4
0.3	2.4	4.3	3.2	3.2
Irradiated and annealed (300 °C/50 h)				
0.01	3.0	0.45	0.5	1.2
0.1	4.5	1.4	3.7	2.5
0.2	4.5	1.7	4.5	2.7
0.3	4.0	2.5	5.2	3.1

TEM results on cluster (SFT) density for the as-irradiated as well as irradiated and annealed specimens are summarized in Fig. 5 as a function of irradiation dose. Fig. 5 also shows the dose dependence of the number of vacancies contained in the SFT population present in the as-irradiated as well as irradiated and annealed conditions. The number of vacancies in SFTs, N_V, can be obtained from the relationship [16]

$$N_V = c_S \pi d_S^2 b / 5.2\Omega, \quad (1)$$

where c_S is the concentration of SFTs, d_S is the mean equivalent diameter of SFTs, b (0.256 nm for Cu) is the Burgers vector and Ω is the atomic volume (1.18×10^{-29} m^3 for Cu). The values of N_V are given in Table 1. It is interesting to note here that although the post-irradiation annealing at 300 °C causes a significant decrease in the concentration of SFTs at all doses, the total number of vacancies contained in the SFTs does not seem to decrease except for the specimens irradiated to 0.01 dpa. On the contrary, in specimens irradiated to doses higher than 0.01 dpa (i.e. 0.1–0.3 dpa) and then annealed at 300 °C for 50 h, the number of vacancies contained in the SFTs has a tendency to increase with increasing dose level (Table 1, Fig. 5(b)). The increase in N_V is particularly marked in the specimen irradiated to 0.3 dpa (see Section 4.1 for discussion).

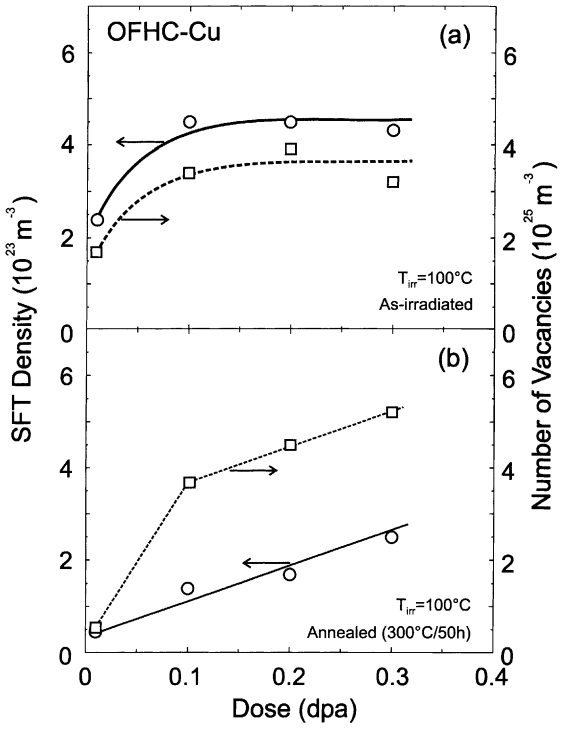

Fig. 5. Dose dependence of SFT density and the number of vacancies contained in the SFTs.

Finally, it should be mentioned that some examples of migration of grain boundaries as well as twin boundaries were found in specimens irradiated to doses $\geqslant$0.1 dpa and then annealed at 300 °C for 50 h. As boundaries migrate, they sweep all the irradiation-induced defects, leaving behind regions free of loops and SFTs.

3.2. Tensile properties

Both as-irradiated and post-irradiation annealed specimens were tensile tested at the irradiation temperature (i.e. 100 °C). The resulting stress–strain curves are shown in Fig. 6. For comparison, the stress–strain curve for the unirradiated copper is also shown in Fig. 6. Clearly, in the as-irradiated samples the yield strength increases very sharply with increasing displacement dose (see Fig. 6(a)). Already at a dose level of 0.01 dpa, the yield strength increases by a factor of 5. At the dose level of 0.3 dpa, the upper yield strength is almost a factor 9 higher than the 0.2% yield strength

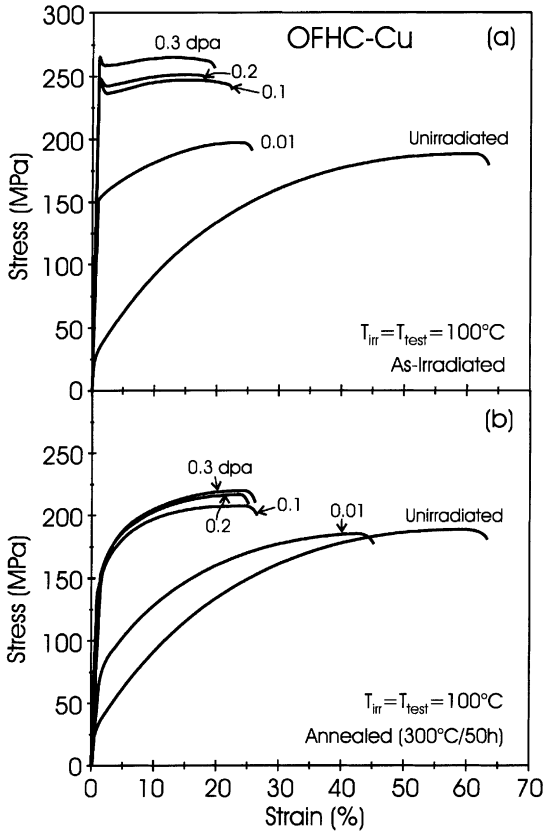

Fig. 6. Stress–strain curves for OFHC-copper (a) in the as-irradiated condition and (b) after post-irradiation annealing at 300 °C for 50 h. Note that the annealing eliminates the occurrence of sharp yield point and subsequent yield drops.

of the unirradiated copper. The increase in strength is accompanied by a severe decrease in the uniform elongation, work hardening ability, and total elongation. Despite this, the failure mode was found to be ductile indicating that the material is not embrittled in a classical sense.

The most interesting features of the results presented in Fig. 6(a) are: (a) the appearance of upper yield point and (b) almost a complete loss of the material's ability to work-harden at doses higher than 0.01 dpa. In fact, the occurrence of an yield point begins already at the dose level of as low as 0.01 dpa (compare the 0.01 dpa curve and the unirradiated curve in Fig. 6(a)). Note that the presence of a distinct yield point, as opposed to the gradual transition to plastic flow in the unirradiated sample, precludes the use of the offset yield strength since the material begins to yield at a clearly defined yield stress. The significance of the yield point and the yield drop is discussed later (Section 4).

The tensile properties of the as-irradiated and irradiated and annealed specimens are given in Table 2. The 0.2% offset yield strength cannot be taken to represent the yield strength of the as-irradiated specimens at dose levels higher than 0.01 dpa because of the yield drop. Hence, the upper yield strength is given for these doses in Table 2. It is interesting to note that the increase in the yield strength due to irradiation begins to saturate above 0.1 dpa, which coincides with the saturation in changes in the microstructure (see Section 3.1).

The effect of post-irradiation annealing (at 300 °C for 50 h) on the tensile behaviour of OFHC-Cu irradiated at 100 °C to different doses is presented in Fig. 6(b). Clearly, the specimens irradiated to 0.01 dpa soften very substantially and become considerably more ductile after annealing. The specimens irradiated to 0.1 dpa and above are less influenced by the post-irradiation annealing. The decrease in the yield strength due to annealing is less than a factor of two for specimens irradiated to 0.1, 0.2 and 0.3 dpa. However, it is significant that in all three cases, the problem of yield drop is eliminated by annealing at 300 °C. Furthermore, the post-irradiation annealed specimens exhibit some reasonable amount of work hardening as well as uniform elongation. It is interesting to note that no yield point is present in the annealed 0.3 dpa specimen (Fig. 6(b)) even though the cluster density is the same as that in the as-irradiated 0.01 dpa specimen and the average cluster size is larger.

In order to facilitate the discussion of irradiation-induced hardening, the dose dependence of the upper yield stress (σ_y^u) and 0.2% offset yield stress ($\sigma_{0.2}$) is presented in Fig. 7 for the as-irradiated and irradiated and annealed OFHC-Cu. In both cases, the yield stress increases rapidly up to a dose level of 0.1 dpa. Beyond this dose level, there is a very small increase in the yield stress with increasing dose level.

3.3. Post-deformation microstructure

The post-deformation microstructures described in this section refer to the microstructures present in the tensile specimens after they had fractured during tensile tests. Specimens irradiated to only the lowest (0.01 dpa) and the highest (0.3 dpa) dose levels were investigated for the deformed microstructures in the as-irradiated and post-irradiation annealed conditions. Fig. 8 shows micrographs of specimens irradiated to 0.01 dpa and then tensile tested in the as-irradiated condition at 100 °C. Although the plastic deformation in the 0.01 dpa specimen occurs mainly in a homogeneous fashion (Fig. 8(a)), the presence of cleared channels were frequently observed (e.g. Fig. 8(b)). Some of the cleared channels were found to be completely free of defect clusters but there were others that still contained a sizeable population of defect clusters. Furthermore, deformation-induced dislocations were found to be present in the volume of materials between the channels. The width of the cleared channels varied between about 100 and 250 nm.

The deformation microstructure in the 0.3 dpa specimens tested in the as-irradiated condition was substantially different from that in the 0.01 dpa specimens. In the case of 0.3 dpa specimens, the deformation

Table 2
Tensile properties of OFHC-copper tested at 100 °C in the unirradiated, as-irradiated and post-irradiation annealed conditions

Dose (dpa)	Post-irradiated annealing	σ_y^u (MPa)	$\sigma_{0.2}$ (MPa)	σ_{max} (MPa)	ε_u^p (%)	ε_t (%)
Unirradiated		–	30	190	56	63
0.01	No post-irradiated annealing	155	155	195	24	26
0.1		245	–	245	–	23
0.2		250	–	250	–	20
0.3		265	–	265	–	22
0.01	300 °C for 50 h	No distinct	68	170	39	43
0.1		yield point	135	208	25	28
0.2			145	215	24	26
0.3			150	220	23	26

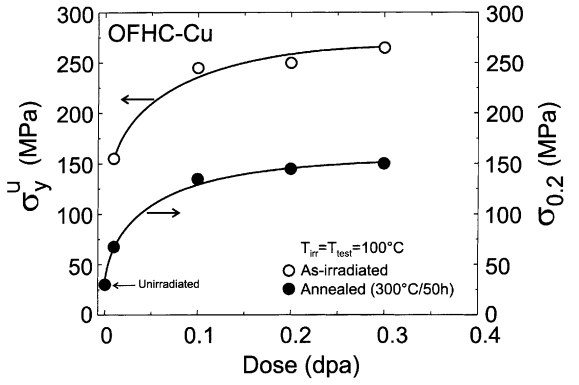

Fig. 7. Dose dependence of the upper yield stress tested in the as-irradiated condition and 0.2% offset yield stress tested in the irradiated and annealed condition.

microstructure in the as-irradiated condition was dominated by the presence of cleared channels, with some dislocation activities in the regions between the cleared channels (see Fig. 9(a) and (b)). TEM observations suggest that at least some of the cleared channels might have originated at the inclusion–matrix interfaces (Figs. 8(b) and 9(b)). The frequency of the cleared channel formation in the 0.3 dpa specimens was considerably higher than that in the 0.01 dpa specimens. The width of cleared channels also in 0.3 dpa specimens varied between about 100 and 250 nm (similar to that in the 0.01 dpa specimens).

Fig. 10 shows the deformation microstructure of 0.01 dpa specimen which was tensile tested after post-irradiation annealing at 300 °C for 50 h. The annealed sample deforms in a homogeneous fashion and exhibits a deformed microstructure similar to the unirradiated copper in which a strong cell structure has developed during deformation (see Fig. 10). There was no clear evidence for the formation of cleared channels in the 0.01 dpa

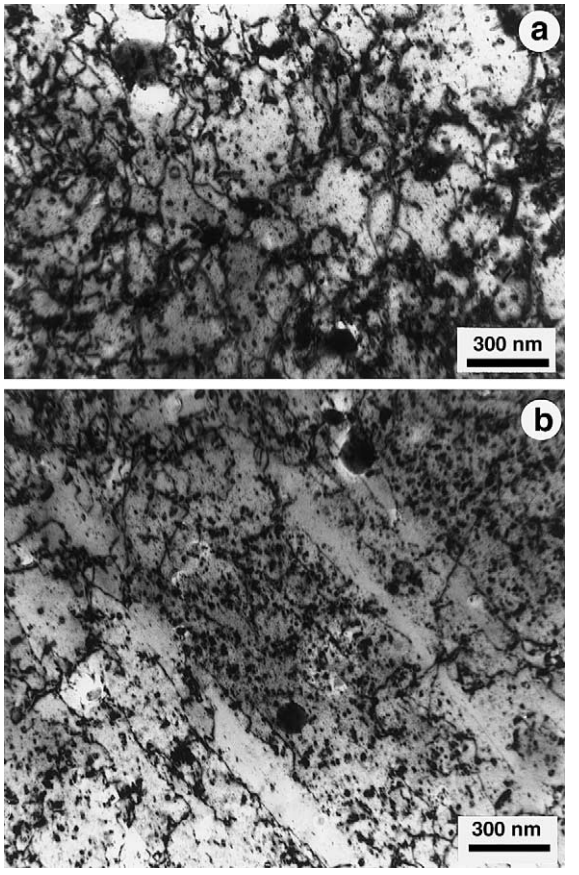

Fig. 8. Post-deformation microstructure of OFHC-copper irradiated at 100 °C to 0.01 dpa and tensile tested in the as-irradiated condition at 100 °C. Note that the deformation occurs both (a) in the homogeneous fashion and (b) localized fashion in the form of 'cleared' channels.

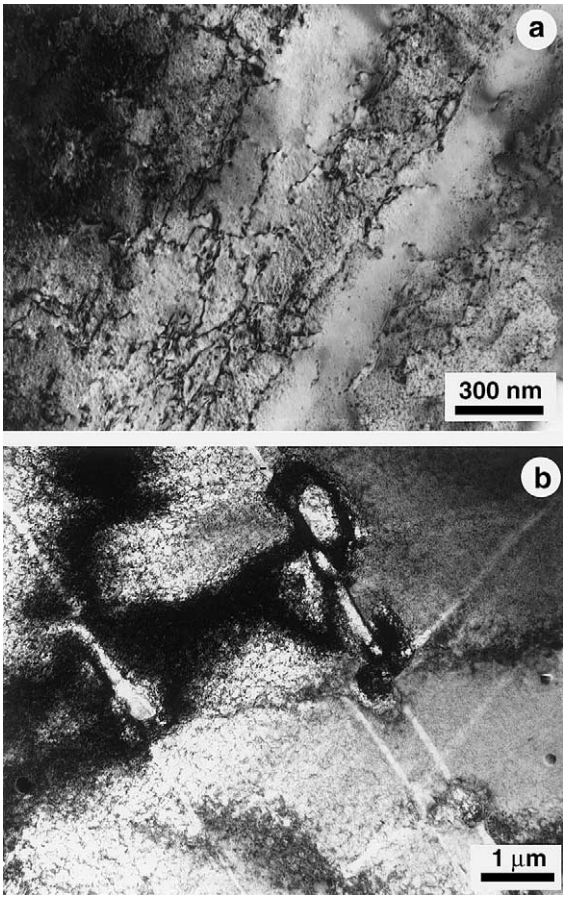

Fig. 9. Same as Fig. 8 but irradiated to 0.3 dpa. Note that some of the cleared channels seem to have originated at relatively large inclusions.

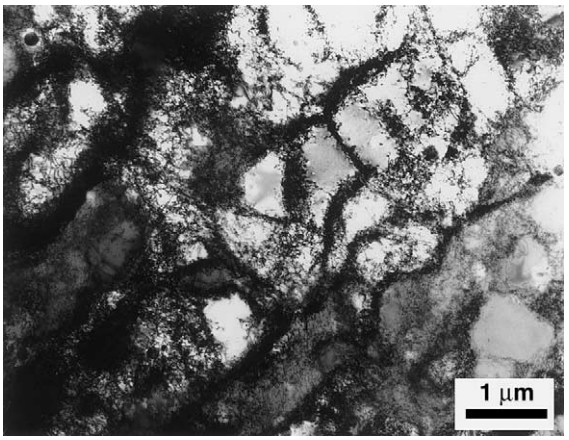

Fig. 10. Post-deformation microstructure of OFHC-copper irradiated at 100 °C to 0.01 dpa and then tensile tested after post-irradiation annealing at 300 °C for 50 h. No cleared channels were observed in these specimens.

annealed specimen tensile tested at 100 °C. However, in some local areas there were indications of the initiation of cleared channels.

Fig. 11(a) and (b) illustrates the deformed microstructures of the post-irradiation annealed sample which was irradiated to 0.3 dpa. The specimen deforms predominantly in a homogeneous fashion (Fig. 11(a)). However, in some regions evidence of localized deformation and cleared channel formation were also observed (Fig. 11(b)).

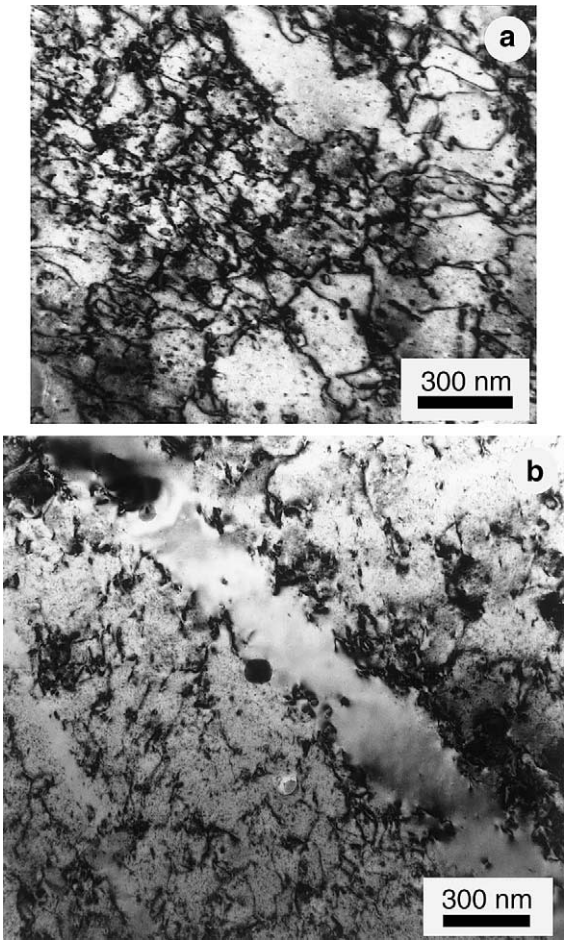

Fig. 11. Same as in Fig. 10 but irradiated to 0.3 dpa. Note that the deformation occurs in (a) homogeneous as well as (b) localized fashion.

4. Discussion

4.1. Microstructural evolution and recovery

The results described in the preceding section suggest that in order to understand the mechanical response of irradiated materials, it is important to understand the evolution not only of vacancy but also of interstitial component of the microstructure as a function of irradiation dose. The results also demonstrate that the annealing kinetics of both vacancy and interstitial type of defect clusters during post-irradiation annealing are affected by the as-irradiated microstructure. The experimental results point to two specific features of the microstructural evolution that should be taken into account while treating the kinetics of annealing of defect clusters and the mechanisms of irradiation hardening and they are:

1. The change in the spatial distribution of interstitial loops from homogeneous to inhomogeneous (i.e. the formation of raft-like agglomerates of loops) with increasing irradiation dose.
2. Although the density of SFTs decreases due to the post-irradiation annealing at 300 °C for 50 h, the number of vacancies contained in the SFTs decreases significantly but only in the specimens irradiated to 0.01 dpa (see Fig. 5).

The problem of the microstructural evolution under cascade damage condition is complicated because of the one-dimensional transport of glissile interstitial clusters (e.g. [17,18]). Further complication arises from the possibility that the one-dimensionally diffusing interstitial clusters may change their direction of motion before reaching a sink (see [18,19]). Recently, it has been shown that these problems can be treated properly within the framework of the production bias model (PBM) (see [18,19] for a review). However, these treatments (i.e. in [5,6,18,19]) have been limited to the void swelling temperature regime (i.e. above the recovery stage V). At present no detailed treatment is available which can describe quantitatively the microstructural evolution in

copper, for example, at 100 °C. The formation of the raft-like agglomerates of interstitial loops at doses beyond 0.01 dpa is, on the other hand, at least qualitatively consistent with the results of analytical calculations predicting decoration of dislocations with small interstitial loops and the formation of rafts of loops during irradiation with cascade-producing projectiles [5,6]. The formation of raft-like agglomerates of loops at higher (>0.01 dpa) doses implies that the grown-in dislocations may also get decorated by small interstitial loops.

As described in Section 3.1, the raft-like agglomerates of loops formed during irradiation to doses of 0.1 dpa and above transform into dislocation segments and a loose network of these segments during the post-irradiation annealing at 300 °C for 50 h. A qualitative explanation of this transformation may be that the closely spaced loops in the raft-like agglomerates of loops interact with each other and get linked via further glide or/and conservative climb, forming dislocation segments. These segments then may interact and form a network.

The results shown in Table 1 and Fig. 4 provide sufficient evidence to conclude that the level of irradiation dose itself has a noticeable impact on the annealing kinetics of SFTs. It can be seen, for example, that only in the case of specimens irradiated to 0.01 dpa a substantial amount (≃70%) of vacancies anneal out during post-irradiation heat treatment at 300 °C for 50 h. This happens primarily via annealing out of about 80% of the SFT population (Table 1) without any significant amount of coarsening of SFTs. In specimens irradiated to higher doses (0.1–0.3 dpa), on the other hand, the decrease in the concentration of SFTs due to annealing seems to be related to some kind of coarsening process with the result that the net number of vacancies contained in the surviving SFTs does not seem to decrease during the post-irradiation heat treatment at 300 °C. If anything, the indication is that the SFTs, for instance, in the 0.3 dpa irradiated specimens collect even more vacancies during annealing.

At present, there is no clear and obvious explanation for this complicated annealing kinetics of SFTs. It is worth pointing out, however, that during irradiation of pure copper in a fission reactor such as DR-3 at Risø, a considerable amount of Ni and Zn atoms will be generated via transmutational reactions (e.g. 0.28% Ni/dpa and 0.26% Zn/dpa) during irradiation [20]. This means that even at the low dose level of 0.01 dpa, a total of 54 ppm of Ni and Zn atoms will accumulate in copper. This impurity level can be taken to be of the same order of magnitude as the residual impurity content of the copper specimens used in the present investigations (≃15 ppm, see Section 2). In other words, neither the accumulation nor the thermal annealing of the vacancy and interstitial clusters may be seriously affected by these impurities produced during irradiation. At the dose levels of 0.1–0.3 dpa, on the other hand, the accumulated amount of impurities will be 540–1620 ppm, respectively. It is quite possible then that these considerably higher levels of impurity atoms may have significant effects on the microstructural evolution process during irradiation and the recovery kinetics during post-irradiation annealing of both vacancy and interstitial type of defect clusters. Clearly, further investigations are necessary to identify and quantify the role of transmutational as well as residual impurity atoms in controlling the microstructural evolution during irradiation and thermal recovery of defect clusters during post-irradiation annealing.

4.2. Hardening and yield drop

The observations showing large increase in the upper yield stress and a marked yield drop in the as-irradiated copper are consistent with the CISH model [1,5]. In other words, during irradiation most of the grown-in dislocations in copper are likely to get decorated by small SIA clusters or loops (see [5,6] for detailed calculations). In view of the fact that raft-like agglomerates of loops are formed throughout the specimens irradiated to 0.1 dpa and above and that the extent of agglomeration increases with increasing dose levels (see Section 3.1), it is distinctly possible that the grown-in dislocations get decorated with an atmosphere of small interstitial loops. This would be consistent with the observations of dislocation decoration and the formation of rafts of loops in neutron irradiated single crystal molybdenum [15] and also with the predictions of the analytical calculations of dislocation decoration [5,6] under cascade damage conditions. This means that when dislocations get extensively decorated, they cannot act as Frank–Read sources until the applied stress acting on the decorated dislocations reaches a high enough value to 'free' the dislocations from their decoration. This level is determined by the spacing between the loops in the decoration, the loop size and the stand off distance between the row of loops (forming the decoration) and the dislocation core [1,5].

Consequently, the initiation of the plastic deformation does not occur until this high stress value is reached and hence an increase in the upper yield stress. Unlike the unirradiated material, the presence of a sharp yield point or yield drop indicates that no significant generation or movement of dislocations occurs until the yield point is reached. The occurrence of the yield drop can therefore be understood in terms of a sudden generation of a large number of dislocations either from some of the weakly locked dislocations or/and at the points of stress singularities where the local stress is considerably higher than the applied stress (e.g. at grain boundary triple points, inclusions etc.). Recently, detailed computer simulations have been carried out to determine the stress levels at which dislocations could be unlocked from their atmosphere [8,21] and the results agree well with the results of analytical calculations reported earlier [1,6].

It is reasonable to suggest that the removal of the yield drop or sharp yield point due to the post-irradiation annealing at 300 °C may be linked directly to a partial or complete annihilation or significant coarsening of the atmosphere of SIA clusters or loops decorating the grown-in dislocation. As described in Section 3.1, both SFTs and interstitial clusters coarsen during annealing at 300 °C and the raft-like agglomerates of loops get transformed into dislocation segments and their loose network. Since SFTs are sessile, their coarsening can only occur via evaporation and growth mechanism (i.e. Oswald ripening). This means that at least some of the vacancies evaporating from SFTs are likely to interact with the interstitial clusters in the decoration, making them shrink to the extent that they may become glissile. Once glissile, these SIA clusters either will be absorbed into the dislocation core or will interact with other loops in the decoration. An even more potent mechanism for the coarsening of the loops in the decoration and the loss of loops to the dislocation is likely to be an increase in the frequency of Burgers vector changes and in the velocity of conservative climb of sessile SIA clusters at the annealing temperature of 300 °C (see [5]). The resulting coarsening of the loops and their loss to the dislocations would cause an increase in the 'stand off' distance [1] and in the spacing between the loops in the decoration. Consequently, the stress necessary to unlock the dislocation from the decoration will decrease (see Eq. (8) in [1]) to such a low level that most of the dislocations in the annealed copper will be operating as dislocation sources leading to global dislocation generation. Under these conditions, the source hardening will be masked by barrier and work hardening [5]. This is what we observe in our experiments.

According to the DBH model, the increase in the shear stress due to irradiation should scale with $(c_S d_S)^{1/2}$ (see Eq. (1) for the definition of these parameters). The experimentally observed change in the yield stress due to irradiation (Table 1) is plotted against $(c_S d_S)^{1/2}$ in Fig. 12 for the as-irradiated as well as post-irradiation annealed cases. The defects included in the calculation of $(c_S d_S)^{1/2}$ are limited to the SFT given that the loops and dislocations are present in much lower densities, and therefore do not contribute significantly to the yield strength. Fig. 12 exhibits two interesting features. First, the irradiation-induced hardening in the as-irradiated samples increases very rapidly with $(c_S d_S)^{1/2}$. This is consistent with earlier results (see Fig. 2 in [12]). Secondly, except for the dose level of 0.01 dpa, the increase in the yield stress at a given value of $(c_S d_S)^{1/2}$ is considerably higher in the case of the as-irradiated than that in the post-irradiation annealed case. Note that the $(c_S d_S)^{1/2}$ values for the post-irradiation annealed samples are nearly as high as that measured in the as-irradiated sample irradiated to doses greater than 0.01dpa,

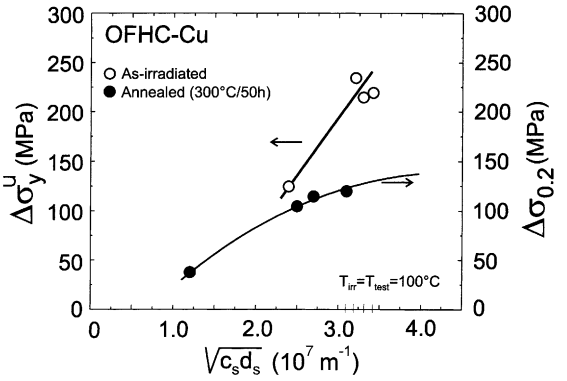

Fig. 12. Variation of irradiation hardening with $(C_S d_S)^{1/2}$.

yet there are clear differences in the tensile behaviour (see the tensile curves in Fig. 6).

The presence of the yield drop and the large discrepancy in yield strength between the as-irradiated and post-irradiation annealed conditions for a given $(c_S d_S)^{1/2}$ value clearly show that the yielding behaviour in the as-irradiated materials cannot be rationalized in terms of DBH model (see [1] for detailed discussion). These differences illustrate that the increase in the yield stress in the as-irradiated specimens is not controlled by the homogeneously distributed SFTs, but rather by some type of pinning of the Frank–Read sources as proposed in the CISH model. In contrast, the yielding behaviour in the post-irradiation annealed samples seems to follow the DBH model where the SFTs and other defects formed after annealing provide resistance to the motion of gliding dislocations. Pinning of the dislocations may still occur in the post-irradiation annealed samples, but does not control the yielding behaviour in a global sense.

The significant amount of recovery that takes place in the specimen irradiated to 0.01 dpa due to annealing at 300 °C for 50 h is qualitatively consistent with the results of Makin [12] for copper irradiated to 4×10^{-3} dpa and annealed at 306 °C for 93 h (Fig. 18 in [12]). However, the rather limited recovery in tensile properties of specimens irradiated to doses of $\geqslant$0.1 dpa and given a post-irradiation annealing treatment at 300 °C for 50 h cannot be explained at present with a high degree of certainty. This limitation arises from the fact that the damage production and accumulation during neutron irradiations are rather complicated even in the case of pure copper since single defects, their clusters and the transmutational impurities (see Section 4.1) are generated continuously and concurrently. Furthermore, the residual impurity atoms as well as transmutational impurities may segregate on the grown-in dislocations and SIA clusters produced during irradiation. The segregation of impurity atoms on SIA clusters may alter their mobility as well as thermal stability. Consequently, the density of accumulated SIA clusters may increase with

dose since transmutational impurities are produced continuously. As described in Section 3.1, during irradiation to doses of 0.1 dpa and above, the clusters and loops form raft-like agglomerates. During the post-irradiation annealing at 300 °C these raft-like agglomerates get transformed into dislocation segments and a network of dislocation is formed in specimens irradiated to doses of 0.1 dpa and above. Naturally, the presence of these dislocations would contribute to the yield strength as well as work hardening.

It could be that the SIA clusters decorated with impurity atoms may act as somewhat harder obstacles to dislocation motion than the 'pure' loops or clusters which may help retain the high strength after post-irradiation annealing (compared to the unirradiated condition). Furthermore, the presence of SFTs is also expected to contribute to hardening, particularly in the case of annealed specimens where deformation occurs homogeneously.

4.3. Plastic flow localization

Finally, let us consider the question of plastic flow localization and cleared channel formation. In this consideration it is important, first of all, to distinguish between the local events such as formation of cleared channels observed in the TEM and the global response of the material reflected in the stress–strain curves obtained during tensile tests. If, for example, during a tensile test the plastic flow localization in the form of cleared channels was to occur only in a small fraction of the total volume of the specimen and concurrently dislocations were generated in the rest of the volume (including the volume between the cleared channels), the stress-strain curve would not be expected to reflect the effect of flow localization since the materials response is dominated by dislocation generation and homogeneous deformation. This is what seems to happen in the case of 0.01 dpa specimens tested in the as-irradiated condition (see Fig. 8) and in the case of 0.3 dpa specimens tested after post-irradiation annealing at 300 °C (see Fig. 11). In contrast, when plastic deformation is overwhelmingly dominated by flow localization in the form of cleared channels and no fresh dislocations are generated in the volume between the channels, the stress–strain curve exhibits a sharp yield point and a yield drop followed by very little or no work hardening. This has been shown to be the case, for example, in copper irradiated at 47 °C to a dose level of 0.2 dpa and deformed at $\simeq$22 °C [22]. In the present experiment, copper specimens irradiated at 100 °C to 0.3 dpa and tested in the as-irradiated condition at 100 °C exhibit a mixed behaviour. The stress–strain curves (Fig. 6) clearly show, for instance, the occurrence of yield drop and the post-deformation microstructure (Fig. 9) illustrates the formation of cleared channels. However, Fig. 6 also shows that the yield drop is followed by a reasonable amount of work hardening which must be caused by homogeneous generation and interactions of dislocations. This is consistent with the post-deformation microstructure shown in Fig. 9 which provides the evidence for some limited amount of dislocation activities in the volume between the cleared channels. In other words, in copper specimens irradiated (to 0.3 dpa) and tested at 100 °C, the plastic deformation is initiated in a localized fashion, but after the yield drop the deformation continues in a mixed mode such that dislocation activities both in the cleard channels as well as in the volume between the channels contribute to the plastic strain.

From the practical application point of view, it is, of course, important that the post-irradiation annealing eliminates the problem of yield drop and reinstates enough uniform elongation to render the material useful again. This points to the possibility that in-service annealings during reactor shut downs might be useful in containing the problem of loss of ductility and may help increase the service lifetime of copper-based components in a fusion reactor. However, the fact that the annealing of specimens irradiated to dose levels of $\geqslant$0.1 dpa shows only a limited amount of recovery in strength and ductility and provides evidence for localized deformation in the form of 'cleared' channels suggesting that caution should be exercised in drawing optimistic conclusions from the present results. It could be, for example, that the re-irradiation of the partly recovered materials may once again induce an increase in the yield stress leading to yield drop and decrease in uniform elongation, but the dose dependence of this behaviour is unknown. This uncertainty needs to be resolved by experimental investigations using several cycles of irradiations and post-irradiation annealings.

5. Conclusions

On the basis of the present results and their discussion, the following conclusions can be drawn:

- In the as-irradiated specimens, formation of raft-like agglomerates of loops is observed at doses above 0.01 dpa, and these agglomerates grow with increasing dose. Post-irradiation annealing transforms these agglomerates into dislocation segments.
- Almost 80% of the SFT population in the specimen irradiated to 0.01 dpa is annealed out during post-irradiation annealing at 300 °C for 50 h. However, in specimens irradiated to higher doses (0.1–0.3 dpa), the post-irradiation heat treatment does not cause any net reduction in the number of vacancies contained in the SFTs. On the contrary, the SFTs exhibit a tendency to acquire additional vacancies during annealing.
- The post-irradiation annealing at 300 °C for 50 h (following irradiation at 100 °C) causes only a partial

recovery in the yield strength. Neither the yield stress nor the uniform elongation recover to the level observed in the unirradiated specimens. The magnitude of the recovery is found to be dependent on the displacement dose level.

- The post-irradiation annealing eliminates the problem of yield drop in OFHC-copper and reinstates enough of uniform elongation to render the materials potentially useful again.
- During deformation cleared channels are formed in all specimens both in the as-irradiated and post-irradiation annealed conditions except for the specimen irradiated to 0.01 dpa and then annealed at 300 °C. The frequency of cleared channel formation increases with increasing yield stress.
- More detailed and systematic experiments are necessary to identify the appropriate mechanism(s) responsible for causing recovery in OFHC-copper.
- The presence of the yield drop in the as-irradiated specimens and the subsequent disappearance of the yield drop after post-irradiation annealing strongly indicate that the Frank–Read sources were pinned in the as-irradiated samples.
- It is pointed out that the effect of transmutatinal impurities (e.g. Ni and Zn) on the microstructural evolution during irradiation and the recovery kinetics of both vacancy and interstitial type clusters during post-irradiation annealing need to be carefully evaluated.

Acknowledgements

The present work was partly funded by the European Fusion Technology Programme. The authors wish to thank B.F. Olsen and J.L. Lindbo for their technical assistance. D.J.E. would like to thank Risø National Laboratory for the support and assistance during his visits. His work was also partly supported by the US Department of Energy under contract DE-AC06-76RLO 1830 with the Battelle Memorial Institute at the Pacific Northwest National Laboratory.

References

[1] B.N. Singh, A.J.E. Foreman, H. Trinkaus, J. Nucl. Mater. 249 (1997) 103.
[2] M. Victoria, N. Baluc, C. Bailat, Y. Dai, M.I. Luppo, R. Schaublin, B.N. Singh, J. Nucl. Mater. 276 (2000) 114.
[3] A. Seeger, in: Proc. Second UN Internat. Conf. on Peaceful Uses of Atomic Energy, Geneva, Septemper 1958, vol. 6, 1958, p. 250.
[4] E. Orowan, Nature 149 (1942) 643.
[5] H. Trinkaus, B.N. Singh, A.J.E. Foreman, J. Nucl. Mater. 249 (1997) 91.
[6] H. Trinkaus, B.N. Singh, A.J.E. Foreman, J. Nucl. Mater. 251 (1997) 172.
[7] N.M. Ghoniem, B.N. Singh, in: J.B. Bilde-Sørensen, J.V. Carstensen, N. Hansen, D. Juul Jensen, T. Leffers, W. Pantleon, O.B. Pedersen, G. Winther (Eds.), Proc. 20th Risø Internat. Symp. on Materials Science, Deformation-Induced Microstructures: Analysis and Relation to Properties, Risø National Laboratory, Denmark, 1999, p. 41.
[8] L.Z. Sun, N.M. Ghoniem, S.-H. Tong, B.N. Singh, J. Nucl. Mater. 283–287 (2000) 741.
[9] Yu.N. Osetsky, A. Serra, V. Priego, J. Nucl. Mater. 276 (2000) 202.
[10] Yu.N. Osetsky, D.J. Bacon, A. Serra, B.N. Singh, in: MRS Symposium Proceedings, paper no. Z3.4, vol. 653, 2001.
[11] A.H. Cottrell, in: Report of Conf. on the Strength of Solids, University of Bristol, England, Phys. Soc., London, 1948, p. 30.
[12] M.J. Makin, in: W.F. Sheely (Ed.), Radiation Effects, AIME, Metallurgical Soc. Conf., Asheville, NC, Septemper 1965, vol. 37, Gordon and Breach, New York, 1966, p. 627.
[13] M.J. Makin, S.A. Manthorpe, Philos. Mag. 8 (1963) 1725.
[14] M. Eldrup, B.N. Singh, J. Nucl. Mater. 258–263 (1998) 1022.
[15] B.N. Singh, J.H. Evans, A. Horsewell, P. Toft, G.V. Müller, J. Nucl. Mater. 258–263 (1998) 865.
[16] C.A. English, B.L. Eyre, J.W. Muncie, Harwell Report AERE-R-12188, September 1986 (HL 86/1357(C15)).
[17] B.N. Singh, S.I. Golubov, H. Trinkaus, A. Serra, Yu.N. Osetsky, A.V. Barashev, J. Nucl. Mater. 251 (1997) 107.
[18] S.I. Golubov, B.N. Singh, H. Trinkaus, J. Nucl. Mater. 276 (2000) 78.
[19] H. Trinkaus, B.N. Singh, S.I. Golubov, J. Nucl. Mater. 283–287 (2000) 89.
[20] L.R. Greenwood, private communication.
[21] N.M. Ghoniem, S.-H. Tong, B.N. Singh, L.Z. Sun, Philos. Mag. A 81 (2001) 2743.
[22] B.N. Singh, D.J. Edwards, P. Toft, J. Nucl. Mater. 238 (1996) 244.